Crossover from Large to Small Polarons across the Metal-Insulator Transition in Manganites

A. Lanzara, N. L. Saini, M. Brunelli, F. Natali, and A. Bianconi
Dipartimento di Fisica and Unità INFM, Università di Roma La Sapienza, P. A. Moro 5, 00185 Roma, Italy

P. G. Radaelli
Institut Max Von Laue-Paul Langevin, Boite Postale 156, 38042 Grenoble Cedex 09, France

S.-W. Cheong
AT&T Bell Labs., Lucent Technology Inc., Murray Hill, New Jersey 07974
(Received 8 October 1997)

We report Mn K-edge extended x-ray absorption fine structure spectra on $La_{0.75}Ca_{0.25}MnO_3$ up to high momentum transfer across the metal-insulator (M-I) transition. The data show compelling evidence for (i) large or intermediate Jahn-Teller polarons (IJTP), characterized by an anomalous longer Mn-O bond ($\Delta R = 0.09$ Å) in the metallic phase ($T < 170$ K), and (ii) appearance of small JT polarons (SJTP) at $T > 170$ K, characterized by a longer Mn-O bond ($\Delta R = 0.21$ Å), which coexist with the IJTP above the M-I transition and has equal probability in the temperature range of colossal magnetoresistance. [S0031-9007(98)06663-0]

PACS numbers: 71.38.+i, 64.70.Kb, 71.30.+h, 75.30.Mb

It is becoming generally recognized that the presence of polarons in doped manganese-oxide perovskites [1–9] and in doped cuprate perovskites [10–12] plays a key role in their peculiar transport properties involving, respectively, the colossal magneto resistance (CMR) and high T_c superconductivity [10,11]. Polarons in the limit of strong (weak) electron-phonon interactions are called small (large) polarons. The large polarons have an itinerant character due to their small effective mass ($m^* \sim 2$–4), and the lattice distortion extended over a wide spatial range. On the other hand, the small polarons could move only by tunneling or thermally activated hopping between locally distorted lattice sites because of the large effective mass ($m^* \sim 10$–100) and the distortion of the lattice extended over a domain of one or few atomic sites.

For an intermediate electron-lattice coupling, such as in doped perovskites, a crossover from large to small polaron regime is expected to be associated with a metal-to-insulator transition. In this regime complex phases could appear with the presence of (a) intermediate polarons having effective mass $m^* = 5$–10 and radius ~ 5 Å and (b) a microscopic phase segregation into domains of itinerant large polarons and localized small polarons [1]. A transition from large to small polarons in the doped manganites in the region around the metal to insulator transition temperature, T_c has been indicated by an anomalous temperature dependence of atomic Debye-Waller factors and lattice parameters [2,3], the infrared spectra [5], the pair distribution function analysis of neutron powder diffraction of the O-O pairs at 2.75 Å [6,7], and the isotrope shift [8,9]. Moreover, there are experimental evidences for spatial ordering of polarons in charge stripes [13,14] and ferromagnetic metallic domains of about 15 Å [15,16].

The polarons in manganites have been interpreted as Jahn-Teller (JT) polarons where the JT stabilization energy is comparable with the bare conduction bandwidth [4,17]. In doped $La_{1-x}Ca_xMnO_3$ the electronically active orbitals are the Mn $3d$ orbitals and mean number of electrons per Mn is $4 - x$. Three electrons go into the t_{2g} core states and the remaining $1 - x$ electrons go into a band of width ~ 2 eV made mostly of outer shell e_g orbitals. In the limit of small polarons localized on one atomic site, the energy of Mn sites with one e_g electron ($1 - x$ Mn^{3+} ions) is lowered by spontaneous distortion of the surrounding lattice: the Jahn-Teller effect. On the contrary, the sites with no e_g electrons (x Mn^{+4} ions) will be associated with an undistorted Mn site structure.

The JT distortion of Mn^{3+} ion is an axial elongation of two Mn-O bonds of the MnO_6 octahedra giving a splitting to the e_g states. Thus, for a compelling experimental evidence of polarons in the CMR materials, it is necessary to have a direct measurement of the following: (1) The axial Mn-O bond length elongation measuring the polaron JT stabilization energy and (2) the probability P of the instantaneous JT distorted Mn sites. The Mn K-edge extended x-ray absorption fine structure (EXAFS) is a fast (10^{-15} s) and atomic selective tool that provides the statistical distribution of instantaneous bond lengths and well-suited probe to these parameters. Tyson *et al.* [18] have used EXAFS to measure the changes from a symmetric at ($T_1 < T_c$) to the asymmetric distribution of Mn-O distances at temperature ($T_2 > T_c$). Their findings are consistent with a small polaron formation above T_c; however, it was not possible to extract quantitative information because of the limited k range ~ 3–13 Å^{-1} of EXAFS oscillations. On the other hand, the EXAFS work by Booth *et al.* [19] was focused

 0031-9007/98/81(4)/878(4)$15.00

on the temperature dependence of the effective Debye-Waller factors of Mn-O pairs providing a support for the polaron formation across the metal-insulator transition.

The present work is motivated to provide a quantitative measure to the JT polaronic distortion of the MnO_6 octahedra and the probability of the JT distorted and undistorted Mn sites in a wide temperature range covering the metal-insulator phase transition of the $La_{0.75}Ca_{0.25}MnO_3$ system. The EXAFS spectra with high signal to noise ratio up to high momentum transfer ($Q = 2k_{max} = 38$ Å^{-1}) have been recorded using the high brilliance source at the 6 GeV storage ring of European Synchrotron Radiation Facility (ESRF) at Grenoble combined with the fluorescence detection mode to separate directly the partial cross section for transitions from the Mn 1s level. These technical improvements have helped us to achieve the high signal-to-noise ratio and to extend the k range of EXAFS oscillations. By this approach we have obtained a higher resolution for local structure determination that gives a quantitative and direct information about the polaronic distortions. The outcome of the present work is that the small JT polarons (SJTP) coexist with the intermediate JT polarons (IJTP) with the same probability, in the CMR regime, and by decreasing the temperature, below the insulator to metal transition, the SJTP disappear, leaving only the IJTP.

The Mn K-edge x-ray absorption measurements were made on a powder of $La_{0.75}Ca_{0.25}MnO_3$ synthesized by the solid state reaction method. The details of the synthesis method and its magnetic and electrical characteristics have been published elsewhere [2,20]. The sample shows the CMR regime above the metal-to-insulator transition at $T_c \sim 240$ K.

The temperature dependent absorption measurements were performed on the beam line BM29 at the ESRF. A Si(111) double crystal monochromator was used with sagital focusing. The sample was placed in a closed-cycle two stage cryostat, and the temperature was monitored with an accuracy of ± 1 K. The spectra were recorded by detecting the Mn K_α fluorescence yield using 13 Ge element solid state detector with about 130 eV energy resolution. Several scans were collected at each temperature to increase the signal-to-noise ratio, and the experiment was repeated in different runs for estimation of the systematic errors. The EXAFS signal was extracted from the absorption spectra using standard procedure and corrected for the fluorescence absorption [21].

Figure 1 shows Fourier transform $|\mathrm{FT}(k^2\chi(k)|$ of the experimental Mn-K edge EXAFS spectra at several representative temperatures. A change in the local structure across the CMR transition is evident directly from the intensity reversal of the FT peaks corresponding to the Mn-La/Ca and Mn-O-Mn backscatterings and the multiple scattering peaks at $R \sim 5.5$ Å.

In complex systems the real pair distribution function (PDF) of the first shell is not given by the Fourier

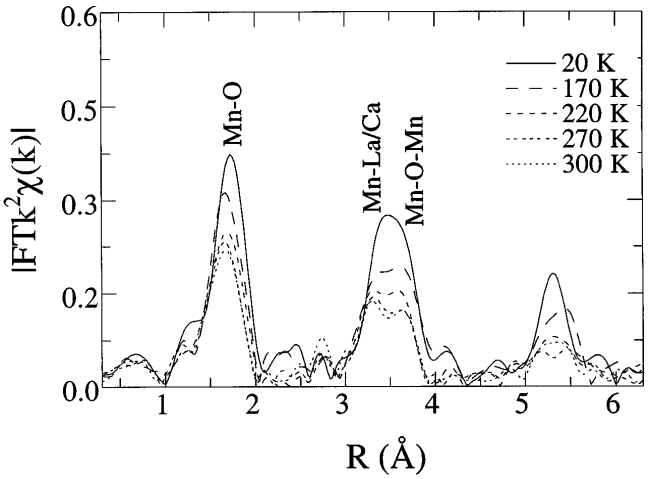

FIG. 1. Magnitude of Fourier transforms, $|\mathrm{FT}(k^2\chi(k)|$, of the Mn K-edge EXAFS recorded at several temperatures. The Fourier transforms are not corrected for the phase shifts and have been performed between $k_{min} = 3$ Å^{-1} to $k_{max} = 19$ Å^{-1} using a Gaussian window.

transform of the raw data. We have used the standard procedures [21,22] to extract the pair distribution function (PDF) of local Mn-O bond lengths from analysis of the EXAFS oscillations due to the Mn-O distances expected in the range 1.8–2.3 Å. The feasibility of these methods has been shown in the case of cuprates [21] and other complex systems [22]. The PDF curves as a function of temperature are shown in Fig. 2(a). The outcome shows an asymmetric distribution of Mn-O bonds peaked around $R_1 \sim 1.92 \pm 0.01$ Å, $R_2 \sim 2.01 \pm 0.01$ Å, and $R_3 \sim 2.13 \pm 0.01$ Å, depending on the temperature. The distribution is a two-peak function with $R_1 \sim 1.92 \pm 0.01$ Å and $R_2 \sim 2.01 \pm 0.01$ Å at low temperature, while a three-peak function in the CMR phase [Fig. 2(b)].

Figure 3 shows the temperature dependence of the Mn-O distance obtained by a weighted average of the pair distribution (Fig. 2) plotted with the Mn-O distance obtained by diffraction measurements (dotted line). The average Mn-O distance shows similar temperature dependence with elongation of the average Mn-O bond lengths in the insulating phase. However, the variation in the Mn-O bonds is bigger at the local scale, indicating that the distortions across the local scale are larger than the one observed by diffraction measurements.

At low temperature, the short distance R_1 in the PDF of Fig. 2 is close to the average crystallographic distance, considering indetermination given by the thermal broadening extracted from diffraction data [2]. The separation between local bond distances, R_1 and R_2 ($\Delta R_p \sim 0.09$ Å), provides the amplitude of instantaneous local lattice distortions due to the dynamic deformations associated with polarons. The polaronic lattice distortion is slightly larger than the indetermination of the bond length due to thermal vibrations $\Delta R_t \sim 0.04$ Å giving a ratio $\Delta R_p/\Delta R_t \sim 2$, indicating the presence of polarons in the

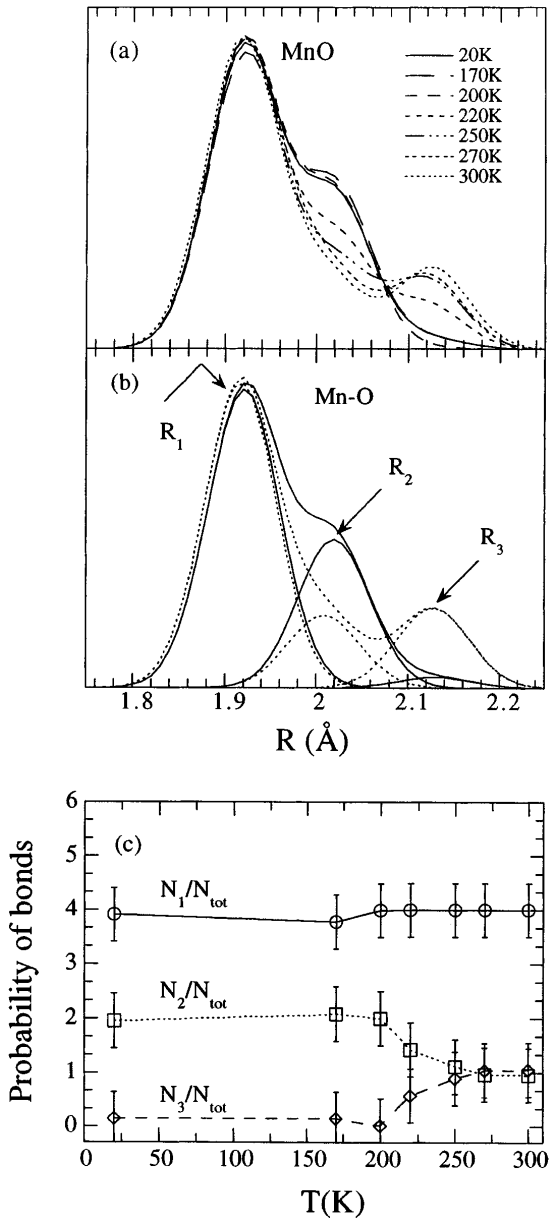

FIG. 2. The Mn-O pair distribution function (PDF) of $La_{0.75}Ca_{0.25}MnO_3$ obtained by analyzing the EXAFS oscillations due to the Mn-O bond lengths; (b) the PDF at 20 and 300 K with their components are plotted for comparison; (c) probability associated with the different bondlengths. The total number of bonds is normalized to 6.

intermediate coupling regime (IJTP) as in the metallic phase of high T_c superconductors [10–12]. Above 170 K a new signal appears in the PDF due to a longer distance $R_3 \sim 2.13 \pm 0.01$ Å. The weight of this signal increases up to a saturation value at the metal-to-insulator transition at $T_c = 240$ K, in the same range the signal due to the R_2 bonds decreases until it reaches the same weight as the R_3.

The temperature dependence of the relative probability of the Mn-O bonds, normalized to 6 (MnO_6 octahedral coordination), is shown in Fig. 2(c). In the metallic

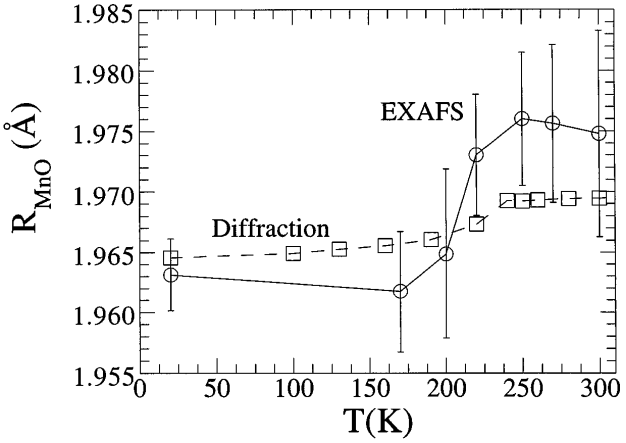

FIG. 3. Temperature dependence of the Mn-O distances. The dashed line is the distance obtained by diffraction on the same sample; the solid line represents the distance obtained by EXAFS.

region ($T < T_c$) the two distances, R_1 and R_2, have a probability of nearly 4 and 2 bonds, respectively. The probability associated with the R_1 remains nearly constant over the temperature range, while the probability of the R_2 gets a value ~1 bond at $T > T_c$ with a crossover temperature $200 < T^* < T_c \sim 240$ K where the long bond R_3 appears with a probability of 1.

The undoped $LaMnO_3$ compound is known to show a spontaneous distortion of MnO_6 octahedra due to the Jahn-Teller effect associated with Mn^{3+} sites. Increasing the concentration of Ca^{2+} ions, an insulator-to-metal transition is observed with a collapse of the difference between crystallographic lattice parameters. However, the local structure in the metallic phase with 25% doping of the Ca^{2+} is expected to diverge from the average crystallographic structure because of local and instantaneous distortions. In fact, the local structure of MnO_6 octahedra contains four in-plane bonds of $\sim 1.92 \pm 0.01$ Å and two out-of-plane bonds of $\sim 2.01 \pm 0.01$ Å showing

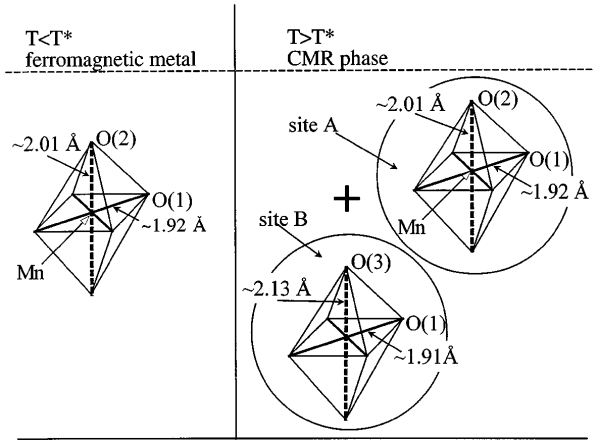

FIG. 4. Pictorical view of the MnO_6 octahedral local distortions in the metallic and insulating phase.

a small Jahn-Teller distortion [Fig. 4(a)]. The ratio $N_2/N_1 \sim 2/4$ of the probability distributions of the two Mn-O bonds (R_2 and R_1) in the metallic phase is consistent with a nearly homogeneous spatial distribution of dynamically axial elongated polaronic MnO_6 octahedra due to overlapping intermediate JT polarons. On the other hand, at $T > T_c$, in the insulating phase the system shows the presence of more elongated MnO_6 octahedra with a longer bond (R_3) such that $\Delta R_p = 0.21$ Å and the ratio $\Delta R_p/\Delta R_t \sim 5$ indicates that the associated polarons are in the strong coupling regime.

We associate this instantaneous lattice distortion with small JT polarons (SJTP). The probability of one very long R_3 bond per Mn site indicates that the SJTP spans about 50% of the Mn sites. Therefore we obtain that in the insulating phase the two distorted sites *A* and *B*, shown in Fig. 4, coexist and each one spans about 50% of the Mn sites. This indicates that the CMR transition is not only accompanied by the appearance of polarons with large amplitude (as observed by other techniques [6–10,15,18–21,23–25]), but also shows a concomitant decrease in the spatial extent of the polaronic charges. It is worth mentioning that the probability of the highly distorted octahedra is twice that of the doping as is the case for the $La_{1.85}Sr_{0.15}CuO_4$ superconducting system [11].

To summarize, we have provided a quantitative characterization of the MnO_6 octahedra of the $La_{0.75}Ca_{0.25}MnO_3$ system. We have found that the metallic state of this system is characterized by homogeneously distributed large polarons while the CMR phase at this exotic metal insulator transition is characterized by the coexistence of small and large polarons. In the CMR phase we find a measure of the size of the small polarons of one hole per two Mn sites, while in the metallic phase the size of overlapping large polarons is at least one hole per 4 Mn sites. These results provide experimental support to the fact that the unusual CMR is related to inhomogeneous and local effects with the formation of small polarons that could form heterogeneous structures at the mesoscopic levels (superlattices) [25]. The measured instantaneous and local lattice distortions provide a base for quantitative calculations of the magnetoresistance mainly via the "double exchange" interactions [4,25,26].

We are happy to acknowledge ESRF staff for their help and cooperation during the Synchrotron beamtime. The work was partially supported by INFM and CNR, Italy.

[1] J. B. Goodenough and J. S. Zhou, Nature (London) **386**, 229 (1997).
[2] P. G. Radaelli *et al.,* Phys. Rev. Lett. **75**, 4488 (1996); P. G. Radaelli *et al.,* Phys. Rev. B **54**, 8992 (1996).
[3] P. Dai *et al.,* Phys. Rev. B **54**, 3694 (1996).
[4] A. J. Millis *et al.,* Phys. Rev. Lett. **77**, 175 (1996).
[5] K. H. Kim *et al.,* Phys. Rev. Lett. **77**, 1877 (1996).
[6] S. J. L. Billinge *et al.,* Phys. Rev. Lett. **77**, 715 (1996).
[7] T. Egami *et al.,* J. Supercond. **10**, 323 (1997).
[8] Guo-Meng Zhao *et al.,* Nature (London) **381**, 676 (1996).
[9] Guo-meng Zhao *et al.,* Phys. Rev. Lett. **78**, 955 (1997).
[10] J. B. Goodenough, J. Mater. Chem. **1**, 715–724 (1991).
[11] A. Bianconi *et al.,* Phys. Rev. Lett. **76**, 3412–3415 (1996), and references therein.
[12] Guo-meng Zhao *et al.,* Nature (London) **385**, 236–239 (1997).
[13] P. G. Radaelli *et al.,* Phys. Rev. B **55**, 3015 (1997).
[14] C. H. Chen and S. W. Cheong, Phys. Rev. Lett. **76**, 4042 (1996).
[15] J. M. De Teresa *et al.,* Nature (London) **386**, 256 (1997).
[16] C. N. R. Rao and A. K. Cheetham, Science **276**, 911 (1997).
[17] K. H. Höck *et al.,* Helv. Phys. Acta **50**, 237 (1983).
[18] T. A. Tyson *et al.,* Phys. Rev. B **53**, 13 958 (1996).
[19] C. H. Booth *et al.,* Phys. Rev. B **54**, 15 606 (1996).
[20] P. Schiffer *et al.,* Phys. Rev. Lett. **75**, 3336 (1995).
[21] N. L. Saini *et al.,* Phys. Rev. B **55**, 12 759 (1997); Physica (Amsterdam) **268C**, 121 (1996), and references therein.
[22] E. A. Stern *et al.,* Phys. Rev. B **46**, 687 (1992); Y. A. Babanov *et al.,* J. Phys. (Paris) **47**, C8-37 (1986); J. Non-Cryst. Solids **79**, 1 (1986).
[23] J. L. Garcia Munoz *et al.,* Phys. Rev. B **55**, 34 (1997).
[24] Y. Yamada *et al.,* Phys. Rev. Lett. **77**, 904 (1996).
[25] A. R. Bishop and H. Röder, Curr. Opin. Solid State Mater. Sci. **2**, 244 (1997); H. Röder *et al.,* Phys. Rev. Lett. **76**, 1356 (1996); J. Zhang *et al.,* Phys. Rev. B **53**, 8840 (1996).
[26] W. E. Pickett and D. J. Singh, Phys. Rev. B **53**, 1146 (1996), and references therein; S. Satpathy *et al.,* Phys. Rev. Lett. **76**, 960 (1996); I. Solovyev *et al.,* Phys. Rev. Lett. **76**, 4825 (1996).